Experimental characterization of the flow and heat transfer inside a horizontal circular tube using C_{60}/tetralin nanofluid

Rita Adrião Lamosa
rita.lamosa@ist.utl.pt

Instituto Superior Técnico, Lisboa, Portugal

November 2019

Abstract

In this work, the flow and the heat transfer of C_{60}/tetralin nanofluid is investigated in a horizontal, circular, smooth, mini-tube with 3.5 mm of inner diameter, under an imposed constant heat flux, for laminar, transition and turbulent flow regimes. Three mass concentrations of nanofluid (0.10%, 0.30% and 0.66 mass%) as well as pure tetralin were experimentally tested at different mass flow rates and at three different inlet temperatures (25°, 35° and 45°C). Temperature and pressure drop measurements were taken, allowing to determine friction factors and convective heat transfer coefficients. It was found that, with temperature raise, the friction factor increased with the mass concentration of the nanoparticles, which represents a penalty on the pumping power. The results also show that the convective heat transfer coefficient was enhanced when comparing data from heat transfer coefficient values plotted against the Reynolds number. However, when comparing the heat transfer coefficients for the same velocity of the flow the results show a decrease in the heat transfer coefficient value for the 0.66 mass% nanofluid. This effect of the addition of C_{60} nanoparticles was attributed to the decrease of turbulence intensity as well as to the increased viscosity of the nanofluids.
Keywords: Nanofluid, Nanoparticles concentration, Temperature, Friction factor, Convective heat transfer coefficient.

1. Introduction

With the increase of environmental concerns the automobile industry has been searching for alternative methods to improve the efficiency of internal combustion engines (ICE). In this kind of engine about 40 percent of the fuel energy is lost in the exhaust system. In order to use this energy with the objective of reducing the CO_2 emissions and improving the thermal efficiency, several waste heat recovery (WHR) systems have been proposed. One of them uses the Rankine Cycle, a cycle based on the steam generation in a secondary circuit.

The most important element in the Rankine Cycle is the heat exchanger (HX). A heat exchanger is a system widely used in engineering applications that allows the transfer of heat between two or more fluids. There are different possible configurations, the one to be implemented is a cross flow tube heat exchanger (figure 1) with the working fluid circulating inside the tubes and the exhaust gases circulating in the exterior [16]. Several studies have been perform so far to develop this heat exchanger. This work further contributes to this main goal, focusing on the properties of the working fluid, by testing it under working conditions closer to those of the real operating heat waste recovery system, being the general working fluid temperatures in the range of 30° to 350°C [15].

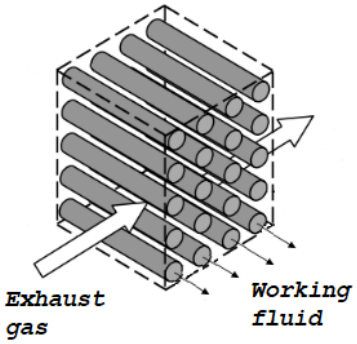

Figure 1: Cross flow HX (adapted from [15]).

It is well known that one of the main limitations in the development of energy-efficient heat transfer medium is the low thermal conductivity of the conventional fluids, such as water or oil [10]. To overcome this issue, several authors suggest the use of nanofluids, i.e. colloidal mixtures of nano-sized particles in a base fluid. This new type of fluid have

heat transfer characteristics superior to both of the base fluid and suspend particles. It offers a compact, green approach when high thermal loads are in demand, having many potential applications from an engineering point of view [14]. A substantial increase in liquid thermal conductivity, heat capacity and heat transfer coefficients are currently reported in the literature when using nanofluids. However, an increase in nanoparticles concentration is also known to often increase the viscosity of the bulk solution, which can lead to several issues related to the fluid flow and to pressure losses [13, 10].

So, the main objective is to evaluate the potential use of nanofluids as working fluid, inferring on the potential advantage of the enhanced thermal properties of such fluids with the possible disadvantage of increased pressure losses due to the augmented viscosity.

In the present study the nanofluid used is a mixture of fullerene particles, C_{60}, and tetralin. Fullerene is an allotrope of Carbon, one of the many forms that carbon based materials can assume. It is a substance produced naturally, in small quantities, that was discovered in 1985 [7], being the Buckminsterfullerene (C_{60}) the most common form to find. Its unique cage structure allows an interesting interaction with solvents, having the capability of dissolving in common organic solvents.

Tetralin, (1,2,3,4-Tetrahydronaphthalene) is a hydrocarbon. It is composed entirely by carbon and hydrogen, having the chemical formula of $C_{10}H_{12}$. It is a colorless liquid, with a strong moldy smell. Tetralin has been widely used in liquefaction of coal and biomass and also as coolant in nuclear power plants.

C_{60} particles have a very good solubility in tetralin, which further improve as the fluid temperature increases, as explained in Kozlov et al. [6]. Fullerene particles are very easy to mix with tetralin, forming a stable mixture. Since the stability of the nanofluid is one of the most difficult obstacles to overcome when preparing a nanofluid, as aforementioned, and given it's high potential to be used in heat transfer applications, at reduced costs, tetralin based nanofluids using fullerene nanoparticles are the main nanofluids which were used in the present work.

2. Nanofluids

This new kind of thermal-fluid has superior thermal properties, as the suspended particles enhance the heat transfer characteristics of the base fluid. In the past few years, a large number of studies have been carried out to investigate nanofluids. Many of them focus on nanofluid development, preparation techniques and characterization, others in heat transfer enhancement, convection, applications and challenges [10, 14, 13, 17, 1].

The addition of nanoparticles changes the thermophysical properties of the base fluid, allowing to artificially tune them for a specific application. The most important properties to tune are thermal conductivity, viscosity, density and specific heat.

Since thermal conductivity of the particles is higher than that of the base fluid, an enhancement of the thermal conductivity of the nanofluid is expected to occur. This enhancement depends on some factors related with particle motion, such as the dispersion of the particles, thermophoresis, diffusiophoresis. Other factors influencing the thermophysical properties of the nanofluid, mostly thermal conductivity and viscosity, are the volume concentration, the shape of the particles, the size of the particles, temperature and pH [18, 3].

2.1. Consequences for the fluid dynamics and heat transfer characteristics in internal flows

The variations of the previously explained thermophysical properties of the nanofluids are the factors that influence the hydrothermal characteristics of the nanofluid. The most important parameters to analyze are the heat transfer coefficient, Nusselt number, Prandtl number as well as the pressure losses. Given this, the thermal conductivity will affect directly the Nusselt and Prandtl numbers, fundamental parameters to analyze the heat capacity of the fluid.

The other important parameter to be analyzed, before apply the fluid to a practical case, is the the flow resistance, i.e the pressure drop, which is directly affected by the viscosity of the nanofluid. The increase of the viscosity represents an increase of the pressure drop, which is not desirable, as it means an increase in the pumping power. On the other hand, viscosity directly affects the convective heat transfer coefficient.

Many research has been published for experimental heat transfer characteristics of various types of nanofluids. For forced convection in smooth, horizontal tubes with a constant heat flux applied, Pak and Cho [12], in 1998, studied the turbulent friction and heat transfer of $Al_2O_3/water$ and $TiO_2/water$ nanofluid. Their results showed that heat transfer increased with increasing volume concentration: for 1.34% volume of Al_2O_3 particles the enhancement was 45% and 75% at a concentration of 2.78%. At the same concentration the heat transfer enhancement for $TiO_2/water$ was less than that of $Al_2O_3/water$. However, under the condition of constant average velocity, for 3% volume concentration, the heat transfer coefficient was 12% smaller than that of the base fluid.

Li and Xuan [8, 9] studied, in 2002 and 2003, the laminar and turbulent convective heat transfer

and friction factor of $Cu/water$ nanofluid. The suspended particles enhance the heat transfer process, increasing the heat transfer coefficient about 60% for 2.0% volume concentration of Cu nanoparticles.

In 2009, Anoop et al. [2], used Al_2O_3 particles dispersed in water to evaluate the effect of particle size on convective heat transfer in laminar developing region. With the increase in particle concentration and flow rate, the average heat transfer coefficient value was increased. However, for the nanofluid with 45 nm particles, the enhancement was around 25%, while for the nanofluid with the 150 nm particles, for the same conditions, the enhancement was 11%.

The literature review introduced in the previous paragraphs provide the context for the investigation of the effects of adding nanoparticles on the convective heat transfer in a horizontal, circular, smooth tube with constant heat flux condition. Most of the published data show a thermal conductivity and a heat transfer coefficient enhancement with increased particle concentration, being the heat transfer coefficient enhancement more pronounced for flows with high Reynolds number. However, different results of this coefficient were reported depending from the analysis method. On the other hand, a penalty in pumping power for using the nanofluids is also reported, due to the increase of the friction factor.

3. Implementation

The experimental setup used in this study is represented in Figure 2, its main description is summarized bellow.

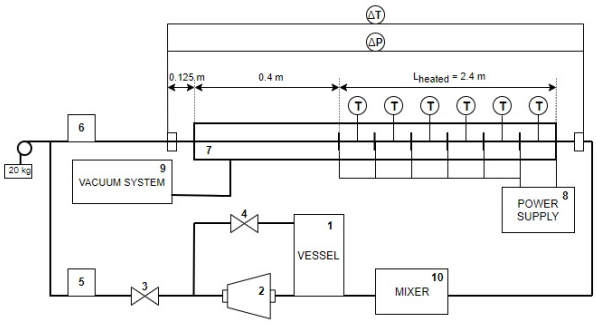

Figure 2: Experimental setup.

The working fluid is introduced in the vessel (1) and is pumped by a magnetically coupled vane pump (2) through the closed loop. The pump is connected to a frequency converter (5) that allows to regulate the flow rate of the working fluid. The flow rate can also be regulated by a bypass valve (4). Once the valve is open it forces the fluid to recirculate to the vessel, reducing the flow in the installation. After the pump, the fluid enters a Coriolis mass flow meter (mini CORI-FLOW M15, Bronkhorst) (6) where the mass flow rate, $\dot{m}$, the inlet temperature, T_i, and the density of the fluid, ρ, are measured. Working in the range of 0.2 to 300 kg/h, with an accuracy of 0.2% and with a density accuracy of 5 kg/m^3. Then, the fluid flows through the test section (7), a smooth round tube with 3.5 mm in inner diameter and 0.25 mm in wall thickness. An initial 0.4 m length without heating is used for flow hydrodynamic developing. The heated area has 2.4 m and is divided into six equal parts with six type K thermocouples (T) installed on the tube wall. A constant heat flux is applied to the walls of this section by a power source (HY5050EX, VOLTEQ)) (8), which allows to regulate the electrical current, I, with an accuracy of 0.5% and the voltage, V, with an accuracy of 0.3% . Also, two thermocouples are placed at the entry and outlet of the test section, which provide the temperature variation in the tube (ΔT). A differential pressure transducer (PX2300, Omega) (ΔP) provides the pressure variation along the test section. To prevent heat loss, the test section is inside a vacuum chamber (9) and all the pipes in the setup are insulated by a rubber insulation. Finally, the fluid enters the mixer, cooler and heating system (10), before returns to the vessel and close the loop. To make sure that the test section is in a horizontal and straight position, a stretching force of 20 kg is used.

All the pressure and temperature signals from the sensors are acquired by a RIGOL acquisition system, connected to a PC with its own software. The data from the Coriolis mass flow meter is processed by the software FlowDDE.

The experimental process consisted in testing four fluids at three different inlet temperatures. The fluids tested were pure tetralin and C_{60}/tetralin nanofluid with 0.10%, 0.30% and 0.66 mass% of nanoparticles. The temperatures at which they were tested were 25°, 35° and 45°C.

3.1. Preparation and characterization of the nanofluids

In this study, particles of fullerene, C_{60} (CAS 99685-96-8) with a purity of 98%, were dissolved in pure tetralin (1,2,3,4-Tetrahydronaphthalene, CAS 119-64-2) to prepare the nanofluid.

The mass fraction of the nanoparticles in the samples was determined by the following equation:

$$w = \frac{m_{np}}{m_{np} + m_{bf}} \tag{1}$$

where m_{np} is the mass of nanoparticles (kg) and m_{bf} is the mass of tetralin (kg). The mass measurements where made in an analytical balance (model ABS80-4N by Kern) with a resolution of 0.1 mg and an accuracy of 0.3 mg.

Figure 3: Nanofluids.

The total mass of tetralin used for the tests in the experimental setup was 1447.448 gr. Table 1 shows the exact mass of C_{60} used for each concentration.

Nanofluid	Mass C_{60} (gr)	Mass fraction (%)
a	1.5005	0.10356
b	4.3485	0.29953
c	9.5475	0.65529

Table 1: Nanofluid concentrations.

Ultrasonication was used to break the nanoparticles cluster and form a well dispersed suspension. The power applied was fixed for the three concentrations, to the value of 35 W.

3.1.1 Thermophysical properties

The density of the nanofluid, ρ_{nf}, is in general considered to be a mixed property of the density of the base fluid, ρ_{bf}, and the density of the nanoparticles, ρ_{np}. So, a widely used equation for this calculation is:

$$\rho_{nf} = \phi\rho_{np} + (1-\phi)\rho_{bf} \tag{2}$$

where ϕ is the particle volume fraction obtained by equation 3, where, respectively, w is the mass fraction of the nanoparticles, obtained by equation 1.

$$\phi = \frac{\frac{w}{\rho_{np}}}{\frac{w}{\rho_{np}} + \frac{1-w}{\rho_{bf}}} \tag{3}$$

The results obtained by the Coriolis mass flow meter were compared and clearly match with the reference data for tetralin [5].

To obtain the dynamic viscosity, a previous analysis to the fluid had to be performed. The dependence of shear stress (τ in Pa) versus shear rate ($\dot{\gamma}$ in s^{-1}) were calculated using the next two equations, respectively:

$$\tau = \frac{D}{4L}\Delta P \tag{4}$$

$$\dot{\gamma} = \frac{32}{\pi D^3}Q \tag{5}$$

Equations 4 and 5 were both used in the laminar flow with no heat flux applied. The results obtained show that C_{60}/tetralin nanofluid is a Newtonian liquid, regardless of the concentration or temperature, and, given this, by implementation of capillary rheometer theory, the equation of viscosity of Hagen-Poiseuille is applicable:

$$\mu = C\frac{\Delta P}{Q} \tag{6}$$

where C is a constant related to the dimensions of the tube and Q is the volumetric flow rate (m^3/s).

The thermal conductivity of tetralin and C_{60}/tetralin nanofluids was measured by the transient hot wire method. There are several techniques which can be used with this purpose, however, the transient hot wire technique is the most used due its accuracy, as it eliminates the errors caused by natural convection in the nanofluid, being very fast compared to other techniques.

The specific heat capacity used in this thesis was obtained by Zhelezny et al. [19, 20].

The relation between each property and the increase in temperature and in mass concentration is present in the following table:

Properties	T ↑	w ↑
Density, ρ	↓	↑
Viscosity, μ	↓	↑
Thermal conductivity, k	↓	×
Specific heat, Cp	↑	↓

Table 2: Relation of thermophysical properties with temperature and mass concentration.

3.2. Data reduction

The thermophysical properties of the four tested fluids, i.e. density ρ, dynamic viscosity μ, thermal conductivity k and specific heat capacity Cp, were evaluated at the mean temperature of the fluid ($\overline{T}$):

$$\overline{T} = Ti - \frac{\Delta T}{2} \tag{7}$$

where ΔT is the temperature difference between the outlet and inlet temperatures of the tube, $\Delta T = T_o - T_i$.

The Reynolds number was calculated with:

$$Re = \frac{4\dot{m}}{\mu\pi D} \tag{8}$$

The friction factor was calculated using the Darcy-Weishbach equation:

$$f = \frac{2D\Delta P}{\rho U^2 L} \tag{9}$$

where U is the mean velocity of the flow, calculated by:

$$U = \frac{\dot{m}}{\rho A_c} \tag{10}$$

where $A_c = 9.6486$ mm^2 is the cross section area of the tube ($A_c = \pi D^2/4$).

The thermal power transferred to the fluid is given by:

$$q = \dot{m} Cp \Delta T \tag{11}$$

which divided by the surface area of the heated length of the tube, $A = 0.026427$ m, ($A = \pi D L_{heated}$) allows to calculate the heat flux, $q'' = q/A$. The heat transfer coefficient is then given by:

$$h = \frac{q}{(\overline{T_s} - \overline{T})} \tag{12}$$

where $\overline{T_s}$ is the surface mean temperature and is calculated by an average of the temperature values of each six thermocouples installed on the tube wall.

$$\overline{T_s} = \frac{T_1 + T_2 + T_3 + T_4 + T_5 + T_6}{6} \tag{13}$$

Then, a number of dimensionless numbers are calculated, which are relevant to analyze the flows of the nanofluids, namely, the Nusselt number;

$$Nu = \frac{hD}{k} \tag{14}$$

Prandtl number:

$$Pr = \frac{\mu Cp}{k} \tag{15}$$

Grashof number:

$$Gr = \frac{g\beta(\overline{T}_s - \overline{T})D^3}{\nu^2} \tag{16}$$

Richardson number:

$$Ri = \frac{Gr}{Re^2} \tag{17}$$

Colburn j-factor:

$$j = \frac{Nu}{RePr^{1/3}} \tag{18}$$

4. Results

4.1. Flow conditions

To assess the flow conditions inside the tube, hydrodynamic and thermal entry lengths were calculated.

The hydrodynamic entry length just depends on the tube diameter and on the Reynolds number, not being affected by the type of fluid used. It was concluded that for laminar and turbulent regions, the flow will be hydrodynamically fully developed, regardless of the concentration of the nanofluid being used.

For the thermal entry length, properties of the flow affect this value in the laminar flow regime, as the thermal entry length in this region depends on the Prandtl number. However, for all the tests carried in this study, the results are similar, so, in the laminar region the flow will be developing thermally. For the turbulent region, the flow will be fully developed thermally.

4.2. Convective analysis

The convection type in the flow was identified based on the Richardson number method. The four fluids were evaluated at the three inlet temperatures, and, for all cases, the Richardson number is smaller than 0.1, meaning that only forced convection is present in the flow.

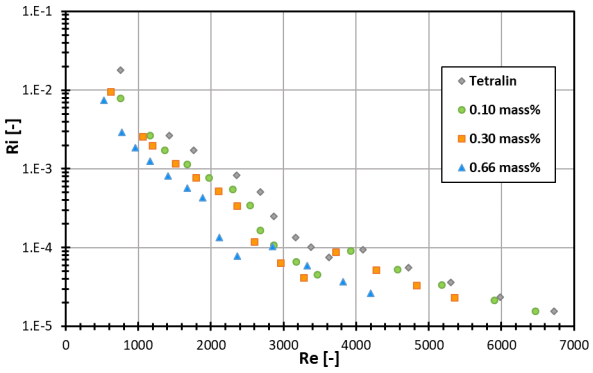

Figure 4: Richardson number versus Reynolds number as a function of nanoparticles mass fraction, at $T_i = 45^oC$.

4.3. Thermal losses

The experimental setup allows to apply an imposed and fixed heat power and therefore a heat flux value (q''_s) to the test section. However, due to thermal losses to the surroundings, the actual heat rate that is transferred to the working fluid is less than the imposed one. The results obtained for the efficiency of the nanofluid show that for all the cases, the efficiency increases as the Reynolds number increases tending to stabilize in the turbulent flow. However, as the temperature increases, the efficiency tends to decrease, specially in the laminar flow.

Also, the efficiency tends to increase as the concentration of the nanofluid increases. These results can be explained, not by the specific heat capacity of the nanofluids, as expected, but by the effects of the viscosity and the density of the nanofluid.

Re	Thermal efficiency [%] 25°C	35°C	45°C
≈1300	85.69	83.83	81.63
≈2500	89.52	86.52	85.28
≈5000	91.61	90.38	90.56

(a) Thermal efficiency obtained for the 0.10 mass% nanofluid at different flow regimes and inlet temperatures.

Re	Thermal efficiency [%] Tetralin	0.10%	0.30%	0.66%
≈1400	85.52	85.69	86.59	87.68
≈2400	86.62	88.32	90.69	92.08
≈5000	90.74	91.61	91.89	95.46

(b) Thermal efficiency of all the working fluids at different flow regimes for $T_i = 25°C$.

Figure 5: Thermal efficiency obtained for the working fluids at different experimental conditions.

4.4. Hydrodynamic characteristics.
4.4.1 Pressure drop

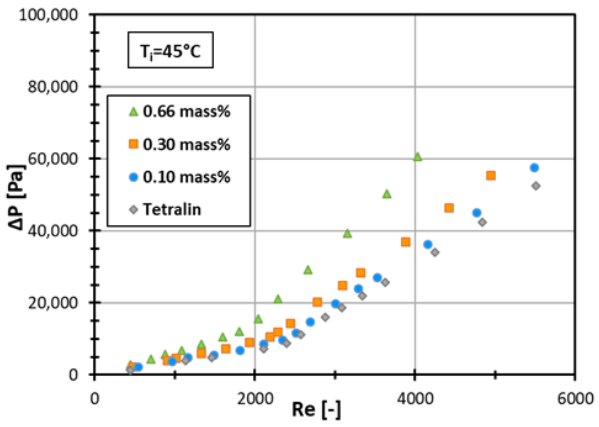

Figure 6: Pressure drop versus Reynolds number as a function of nanoparticles mass fraction at $T_i = 45°C$.

As previously explained, the pressure drop is an important factor when analyzing an internal flow since it directly affects the required pumping power. Since the viscosity of the nanofluids increases with the nanoparticles mass fraction, the pressure drop is larger for an increased concentration of the nanoparticles. Becoming this difference, when compared to pure tetralin, more significant at larger inlet temperatures. This trend can be related to the viscosity of the fluids, since the viscosity decrease with the temperature is not exactly the same for all the nanofluids tested. In fact, a divergence between the curves of tetralin and nanofluids with lower nanoparticles concentration and the nanofluid with the largest nanoparticles concentration was observed, which shows an overall larger viscosity, that tends to decrease less with temperature.

4.4.2 Friction factor

Shown in figure 7 are the obtained values of friction factor for 0.10 mass%, 0.30 mass%, 0.66 mass% C_{60}/tetralin nanofluids and pure tetralin for the entire flow range at an inlet temperature of 45°C. The results are compared with Hagen-Poiseuille and Blasius equations.

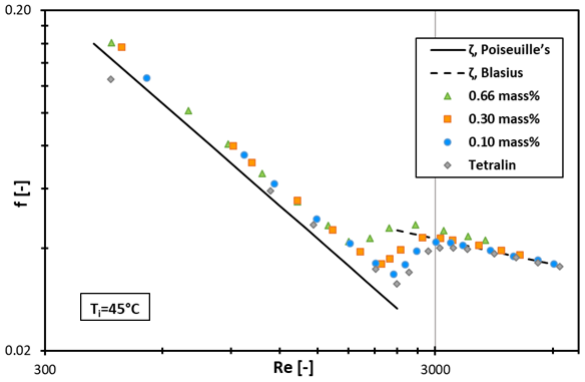

Figure 7: Friction factor versus Reynolds number as a function of nanoparticles mass fraction, at $T_i = 45°C$.

Analyzing the results with more detail, it is possible to notice that, in the laminar flow regime, the friction factor does not depend of the particles concentration, being the values of the friction factor versus Reynolds number the same as for pure tetralin. The largest difference obtained between the nanofluids and tetralin was about 4% for an inlet temperature of 45°C.

The difference in the friction factor between the nanofluids and the tetralin is slightly larger in the turbulent flow, particularly as the inlet temperature and the nanoparticles concentration increases. Hence, the largest values of the friction factor were obtained for the 0.66 mass% nanofluid, at 45°C, which was observed to be about 8.8% larger, for a Reynolds number of 3600, when compared to that of tetralin. This trend can be explained by the viscosity of the nanofluids, as discussed in the previous paragraphs. However, since as the temperature increases, the dynamic viscosity of the fluids decrease and the difference between them becomes more significant, specially for 0.66 mass% nanofluid, and, since the difference between the density of the nanofluids remains constant with temperature raise, it is possible to conclude that with temperature augmentation, the friction factor will increase with nanoparticles concentration, when compared to that of pure tetralin. At the same time, the Reynolds number, for the same fluid velocity, will be higher for tetralin and for the nanofluids with lower mass concentration. So, the transition from laminar to turbulent seems to occur at lower Reynolds for the nanofluid with larger concentration (even

though that may not be true) and its friction factor values will increase. So, overall one can observe that the friction factor increases with mass concentration of nanoparticles augmentation, being this more pronounced as the temperature increases. These differences are also more prominent in transition and turbulent regimes, which are more affected by viscous and mixture effects.

This analysis reveals that, as the temperature increases, an increase of the mass nanoparticles will cause extra penalty in pumping power when compared to pure tetralin.

As aforementioned, the results also suggest an early transition to the turbulent flow for nanofluids, being this transition as early as the increase of mass concentration of the nanofluid.

4.5. Heat transfer

4.5.1 Convective heat transfer coefficient

The experimental values obtained for the heat transfer coefficient, as a function of the Reynolds number are depicted for an inlet temperature of 45°C in figure 8. The results reveal that in the laminar region the heat transfer coefficient is not affected by the addition of the nanoparticles, having just a slight increase as the Reynolds number increases. However, in the turbulent region, it increases with the increase in mass concentration of the nanoparticles. This augmentation is more pronounced as the temperature increases. For turbulent flow, at a Reynolds number of approximately 4000, the heat transfer coefficient is enhanced by 4.9% when using 0.10 mass% nanofluid, by 11.2% when using 0.30 mass% and 30.5% when using 0.66 mass% nanofluid.

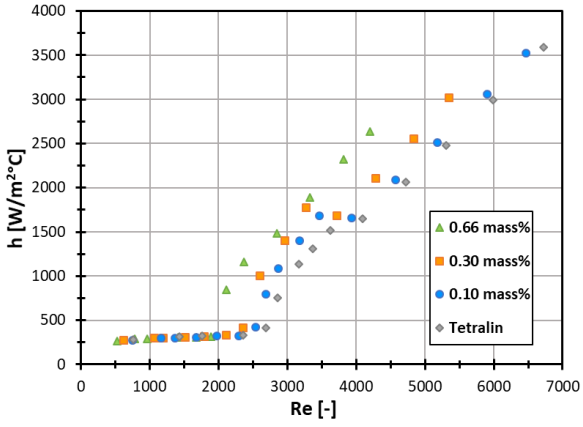

Figure 8: Heat transfer coefficient versus Reynolds number as a function of nanoparticles mass fraction, at $T_i = 45°C$.

However, looking at the evolution of the heat transfer coefficient as a function of the Reynolds number can be deceiving when comparing the different nanofluids, since, as discussed in previous points, the viscosity varies in a different way on temperature, depending on the nanoparticles concentration, which may alter the values of the Reynolds number in a way that disables an accurate comparison between the different fluids. Hence, as an alternative, earlier proposed by Pak and Cho [12] and depicted in figure 9 the heat transfer coefficient obtained for the different fluids can be compared under the condition of constant average velocity, since it gives a more accurate representation of the heat transfer. The results show that for a mean velocity value of 1.5 m/s, the heat transfer coefficient of 0.10 mass% C_{60}/tetralin nanofluid is 1.22% higher, at 0,30 mass% is 2.06% higher and at 0.66 mass% is 8.36% lower than pure tetralin. This slight decrease of the convective heat transfer coefficient can be appreciated in figure 9 and is only valid in the turbulent flow regime.

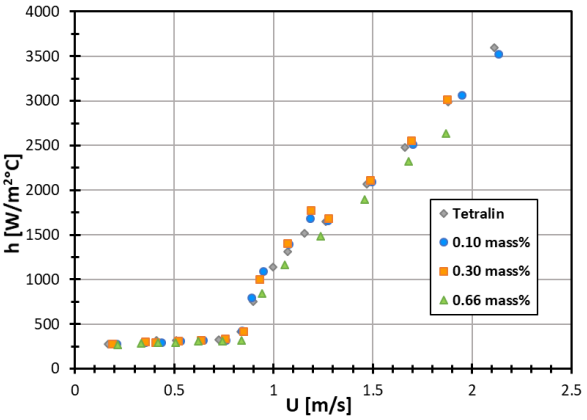

Figure 9: Heat transfer coefficient versus mean fluid velocity as a function of nanoparticles mass fraction, at $T_i = 45°C$.

This decrease of the heat transfer coefficient for the nanofluid with the highest concentration tested can be explained by the findings reported by Rudyak et al.[11] who studied the transition (from laminar to turbulent regime) of a nanofluid flow inside a pipe. Rudyak et al. [11] observed that, with increasing concentration of nanoparticles, the transition occurred at smaller Reynolds numbers. However, Rudyak et al. [11] also measured the pressure pulsations in the tube and observed that in turbulent flow regime, the nanoparticles reduce the pressure pulsations. This reduction leads to a decrease of the small-scale turbulent fluctuations, i.e, a turbulence degree reduction, decreasing the mixing inside the pipe, which results in a lower heat transfer coefficient.

4.5.2 Nusselt number

The Nusselt number was also evaluated for the four fluids at the three different inlet temperatures. As

expected, and in agreement with the results reported in the previous paragraphs, for the same Reynolds number, as the mass concentration of the nanofluid increases, the Nusselt number also increases, being this increase more significant at the highest temperature tested, 45°C, as can be seen in figure 10. The results show a raise of the Nusselt number of about 56% for 0.66 mass% nanofluid, at a Reynolds number of about 4100. However, this augmentation, only affects the turbulent region, not affecting the laminar region neither by the temperature or by the particles concentration.

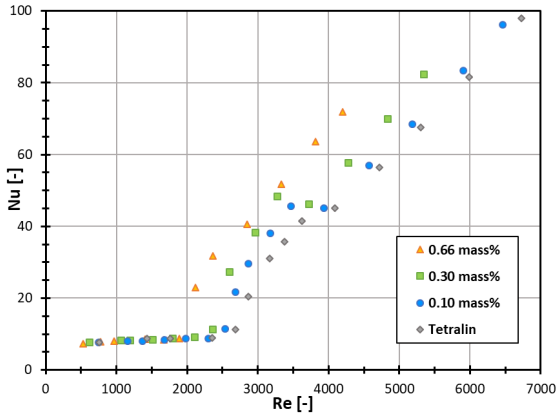

Figure 10: Nusselt number versus Reynolds number as a function of nanoparticles mass fraction, at $T_i = 45°C$.

4.5.3 Colburn j-factor

Considering the subjective determination of the transition region based on the visual inspection of the plots, the Colburn j-factor was used as a complementary parameter, as proposed by Everts and Meyer [4]. Looking at the Colburn j-factor, as a function of the Reynolds number and in agreement with the results discussed in the previous sections, the transition from laminar to turbulent occurs at lower Reynolds numbers, as the mass concentration of C_{60} nanoparticles increases. This trend is more pronounced for higher inlet temperatures. Although these results can be clearly seen in the graphics that have been presented, again care must be taken in their interpretation which is still based on the visual inspection of plots presented as a function of the Reynolds number. Aiming at a more accurate identification of the critical conditions for the occurrence of the transition, the Colburn j-factor gradient as a function of the Reynolds number is evaluated, following the method proposed by Everts and Meyer [4]. Figure 12 shows, as an illustrative example, the obtained Colburn j-factor gradient as a function of the Reynolds number for 0.10 mass% nanofluid for the three inlet temperatures tested.

The closest value as possible of the critical

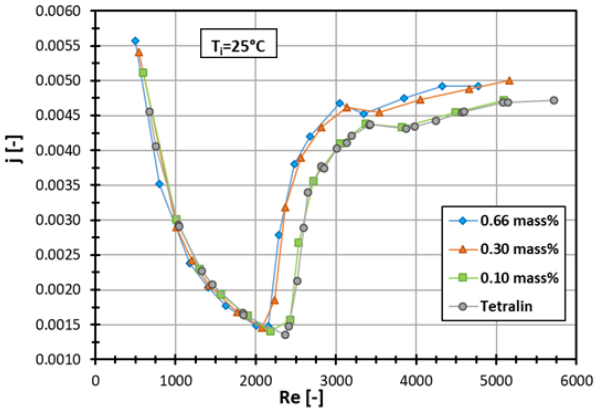

(a)

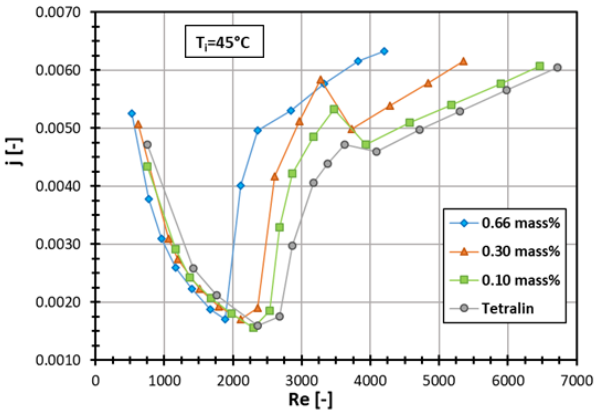

(b)

Figure 11: Colburn j-factor as a function of Reynolds number, at T_i of (a) $25°C$ (b) $45°C$.

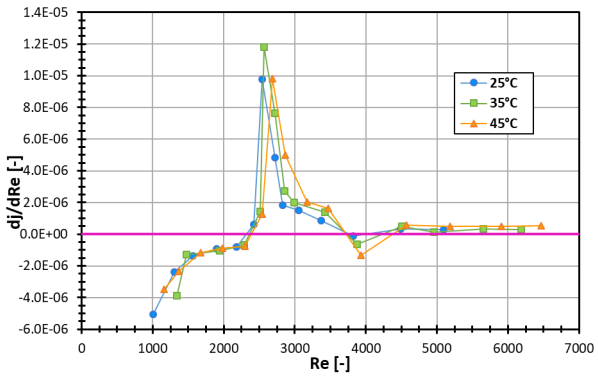

Figure 12: Colburn j-factor gradient versus Reynolds number, as a function of the inlet temperature for 0.10 mass% nanofluid.

Reynolds, Re_{crt}, i.e. the Reynolds for the start of the transition flow regime and end of the laminar flow regime, was obtained as the derivative turns from negative to positive. The obtained values, for tetralin, 0.10%, 0.30% and 0.66 mass% nanofluids at the three different inlet temperatures are sum-

marized in table 3.

	25°C	35°C	45°C
Tetralin	2388	2469	2570
0.10 mass%	2315	2363	2389
0.30 mass%	2113	2253	2231
0.66 mass%	2155	2017	1902

Table 3: Critical Reynolds number.

The results clearly show a decrease of the critical Reynolds number as the nanoparticles mass concentration increases, for all the temperatures tested. This corroborates the previously obtained results discussed when analyzing the pressure drop, the friction factor, the heat transfer coefficient and Nusselt number, of the transition to occur earlier, i.e. at lower Reynolds numbers for the nanofluids, being this as early as the mass fraction of nanoparticles increases.

On the other hand, it is possible to see a general increase of the critical Reynolds number as the temperature increases, i.e, an overall delay in transition, as the temperature increases. Although, for the nanofluid with the highest concentration, 0.66 mass%, the transition starts earlier as the temperature increases. This anticipation of the transition with the temperature raise can be explained again with the dynamic viscosity, following the same arguments used in 4.4.2.

5. Conclusions

The present work was aimed at evaluating the potential benefits of using C_{60}/tetralin nanofluid as a working fluid for a heat exchanger to enhance the heat transfer mechanisms. So, this work presents a study on the effects of adding fullerene nanoparticles on the heat transfer and hydrodynamic behavior on C_{60}/tetralin nanofluid flowing inside a horizontal, circular and smooth tube with a constant heat flux applied. Particular emphasis is given to the effect of increasing the mass concentration of the particles and the inlet temperature of the working fluid.

- Regardless the working fluid, the flow was hydrodynamically fully developed in all Reynolds number range. Thermally developed for turbulent regime and developing in the laminar regime.

- Only forced convection was present in the flow.

- Thermal efficiency tends to increase with mass concentration of C_{60} nanoparticles, as well with the Reynolds number and tends do decrease with temperature raise. This is due to thermophysical properties variation, namely, viscosity and density.

- Friction factor raise with temperature increase and with mass concentration of the nanoparticles increase, representing a pumping power penalty when using the nanofluids.

- On the convective heat transfer coefficient the results depend on the method used to evaluate it. So, the heat transfer coefficient increases with the increasing Reynolds number and with increasing mass concentration of nanoparticles. When comparing the heat transfer coefficients as a function of the mean velocity of the fluid, 0.66 mass% nanofluid showed a decrease of about 8.36%, when compared to pure tetralin, attributed to the reduction in the degree of turbulence.

- Analyzing the Colburn j-factor and its gradient allows to conclude that the transition starts at a lower Reynolds number as the nanoparticles concentration increases. When assessing the influence of the inlet temperature in the transition, the results show a delay in the laminar-turbulent transition with temperature raise, except for the nanofluid with highest concentration, which is explained by the dynamic viscosity.

Using different methods to identify the occurrence of transition allowed to confirm the consistency of the trends evaluated in each method, stressing that the major role of the nanoparticles concentration, for the range studied in the present work, was to alter relevant bulk properties of the fluids, namely the viscosity, which dominated over the variation of other properties such as the thermal conductivity. Overall these effects became dominant leading to a significant increase of the heat transfer coefficient despite of the penalty in the pumping power. So, the use of this nanofluid is recommended as a working fluid with enhanced thermal properties, although the concentration of the nanoparticles should be carefully considered due to the increase pumping power penalty and the deterioration of the heat transfer coefficient for concentration equal or higher than 0.66 mass%.

References

[1] T. Ambreen and M. H. Kim. Heat transfer and pressure drop correlations of nanofluids: A state of art review. *Renewable and Sustainable Energy Reviews*, 91(March):564–583, 2018.

[2] K. B. Anoop, T. Sundararajan, and S. K. Das. Effect of particle size on the convective heat

transfer in nanofluid in the developing region. *International Journal of Heat and Mass Transfer*, 52(9-10):2189–2195, 2009.

[3] W. H. Azmi, K. V. Sharma, R. Mamat, G. Najafi, and M. S. Mohamad. The enhancement of effective thermal conductivity and effective dynamic viscosity of nanofluids - A review. *Renewable and Sustainable Energy Reviews*, 53:1046–1058, 2016.

[4] M. Everts and J. P. Meyer. Heat transfer of developing and fully developed flow in smooth horizontal tubes in the transitional flow regime. *International Journal of Heat and Mass Transfer*, 117:1331–1351, 2018.

[5] F. A. Gonçalves, K. Hamano, and J. V. Sengers. Density and Viscosity of Tetralin and Trans-Decalin. *International journal of Thermophysics*, 10(4), 1989.

[6] A. V. Kozlov, A. M. Kolker, N. G. Manin, and N. I. Islamova. Polythermal study of C60 solubility in tetralin. *Mendeleev Communications*, 17(6):362–363, 2007.

[7] H. W. Kroto, J. R. Heath, S. C. O'Brien, R. F. Curl, and R. E. Smalley. C60 : Buckminsterfullerene. *Letters to nature*, 318:162–163, 1985.

[8] Q. Li and Y. Xuan. Convective heat transfer and flow characteristics of Cu-water nanofluid. *Science in China (Series E)*, 45(4):408–416, 2002.

[9] Q. Li and Y. Xuan. Investigation on Convective Heat Transfer and Flow Features of Nanofluids. *Journal of Heat Transfer*, 125(1):151, 2003.

[10] Y. Li, J. Zhou, S. Tung, E. Schneider, and S. Xi. A review on development of nanofluid preparation and characterization. *Powder Technology*, 196(2):89–101, 2009.

[11] A. V. Minakov, V. Y. Rudyak, D. V. Guzey, M. I. Pryazhnikov, and V. A. Zhigarev. On laminar-turbulent transition in nanofluid flows. *Thermophysics and Aeromechanics*, 23(5):773–776, 2016.

[12] B. C. Pak and Y. I. Cho. Hydrodynamic and heat transfer study of dispersed fluids with submicron metallic oxide particles. *Experimental Heat Transfer*, 11(2):151–170, 1998.

[13] R. Saidur, K. Y. Leong, and H. A. Mohammad. A review on applications and challenges of nanofluids. *Renewable and Sustainable Energy Reviews*, 15(3):1646–1668, 2011.

[14] M. U. Sajid and H. M. Ali. Recent advances in application of nanofluids in heat transfer devices: A critical review. *Renewable and Sustainable Energy Reviews*, 103:556–592, 2019.

[15] H. Santos, D. Caseiro, N. Pires, J. F. Pereira, J. Morgado, and N. Martinho. Experimental Study of an Evaporator Heat Exchanger for a Rankine Cycle Vehicle Waste Heat Recovery System. *Journal of Clean Energy Technologies*, 4(5):362–366, 2015.

[16] H. Santos, J. Morgado, N. Martinho, J. Pereira, and A. Moita. Selecting and Optimizing a Heat Exchanger for Automotive Vehicle Rankine Cycle Waste Heat Recovery Systems. *Energy Procedia*, 107(September 2016):390–397, 2016.

[17] J. Sarkar. A critical review on convective heat transfer correlations of nanofluids. *Renewable and Sustainable Energy Reviews*, 15(6):3271–3277, 2011.

[18] N. Sezer, M. A. Atieh, and M. Koç. A comprehensive review on synthesis, stability, thermophysical properties, and characterization of nanofluids. *Powder Technology*, 344:404–431, 2019.

[19] V. Zhelezny, O. Khyliyeva, and A. Nikulin. Effect of fullerene C60 on heat capacity, density, thermal conductivity and viscosity of tetralin. 165, 2019.

[20] V. Zhelezny, I. Motovoy, O. Khliyeva, and N. Lukianov. Thermochimica Acta An influence of Al2 O3 nanoparticles on the caloric properties and parameters of the phase transition of isopropyl alcohol in solid phase. *Thermochimica Acta*, 671(September 2018):170–180, 2019.